Inhibitors of Aspartate Transcarbamoylase Inhibit Mycobacterium tuberculosis Growth

Du, Xiaochen; Sonawane, Vidhisha; Zhang, Bidong; Wang, Chao; de Ruijter, Bram; Dömling, Alexander S S; Reiling, Norbert; Groves, Matthew R

Published in:
ChemMedChem

DOI:
10.1002/cmdc.202300279

ChemMedChem

Research Article
doi.org/10.1002/cmdc.202300279

Chemistry Europe
European Chemical Societies Publishing

www.chemmedchem.org

Inhibitors of Aspartate Transcarbamoylase Inhibit *Mycobacterium tuberculosis* Growth

Xiaochen Du,[a] Vidhisha Sonawane,[b] Bidong Zhang,[a] Chao Wang,[a] Bram de Ruijter,[a] Alexander S. S. Dömling,*[a, b] Norbert Reiling,*[c, d] and Matthew R. Groves*[a]

Aspartate transcarbamoylase (ATCase) plays a key role in the second step of *de novo* pyrimidine biosynthesis in eukaryotes and has been proposed to be a target to suppress cell proliferation in *E. coli*, human cells and the malarial parasite. We hypothesized that a library of ATCase inhibitors developed for malarial ATCase (*Pf*ATCase) may also contain inhibitors of the tubercular ATCase and provide a similar inhibition of cellular proliferation. Of the 70 compounds screened, 10 showed single-digit micromolar inhibition in an *in vitro* activity assay and were tested for their effect on *M. tuberculosis* cell growth in culture. The most promising compound demonstrated a MIC_{90} of 4 μM. A model of *Mtb*ATCase was generated using the experimental coordinates of *Pf*ATCase. *In silico* docking experiments showed this compound can occupy a similar allosteric pocket on *Mtb*ATCase to that seen on *Pf*ATCase, explaining the observed species selectivity seen for this compound series.

Introduction

Tuberculosis is an ancient disease caused by species of the Mycobacterium tuberculosis complex including *M. tuberculosis* (Mtb), *M. africanum, M. canettii, M. microti, M. caprae, M. bovis*, and *M. pinnipedii*.[1] Of these Mtb has had the largest impact on mankind. It first appeared as a human pathogen around seven thousand years ago in Africa and has evolved continually – spreading throughout the world.[2] In 1993, Mtb was announced to be a global disease by the World Health Organization (WHO), and nowadays this disease remains one of the top 10 causes of death worldwide, with a quarter of all people infected with Mtb globally, and 30 high-risk countries.[3]

Mtb possesses specific characteristics that aid its survival in macrophages of the human host.[4] In addition external factors which could disrupt host-pathogen balance or affect T cell function (such as viral co-infection, particularly HIV) increases the risk of disease progression in latently infected individuals.[2a] A very peculiar feature of Mtb is its very complex cell wall, mainly composed of mycolic acids, lipoarabinomannan, arabinogalactan and peptidoglycans, which represents a very efficient protective barrier against different forms of stress, such as host cell factors but also antibiotics.[5] In addition to Rifampicin (RIF; acting on RNA polymerase),[6] Fluoroquinolones (acting on DNA synthesis),[7] several anti-TB drugs target the cell wall biosynthesis such as isoniazid (INH; acting on mycolic acid biosynthesis[8]), ethambutol (EMB; acting on arabinogalactan biosynthesis[9]), thiolactomycin (TLM; acting on mycolic acid and fatty acid biosynthesis[10]), and D-cycloserine (acting on alanine racemase that is important for the biosynthesis of peptidoglycan layer[11]). However, the increase of patients infected with multidrug-resistant (MDR) and extremely drug-resistant (XDR) Mtb is a major concern highlighting the urgent need for the identification of novel targets and inhibitors, which could be exploited to improve TB treatment. Beside the unique physiological characteristics of Mtb, such as targeting cell wall biosynthesis, druggable candidates are likely to be found in essential pathways, for instance, growth or proliferation, metabolism and energy support systems.[12]

De novo pyrimidine nucleotide synthesis is one of the two pathways for pyrimidine nucleotide production in living organisms and includes six catalytic steps catalyzed by three unique enzymes in humans: CAD (composed of carbamoyl phosphate synthetase II (CPS- II), aspartate transcarbamoylase (ATCase) and dihydroorotase (DHODH)), UMPS (orotate phosphoribosyl transferase (OPRT)) and orotidine monophosphate decarboxylase (OMPDC). The second pathway to supply pyrimidines is through a salvage pathway. Aspartate transcarbamoylase (ATCase) catalyzes the second step of *de novo* pyrimidine biosynthesis, responsible for the formation of carbamoyl-aspartate (CP-ASP) from L-aspartate (L-ASP) and carbamoyl phosphate (CP).[13] The ATCase of *Escherichia coli* was fully characterized and has been

[a] X. Du, B. Zhang, C. Wang, B. de Ruijter, Prof. A. S. S. Dömling, Prof. M. R. Groves
XB20 Drug Design, Groningen Research Institute of Pharmacy
University of Groningen
A. Deusinglaan 1, Groningen 9700AV (The Netherlands)
E-mail: a.s.s.domling@rug.nl
m.r.groves@rug.nl
[b] V. Sonawane, Prof. A. S. S. Dömling
CATRIN, Department of Innovative Chemistry
PalackýUniversity, 779 00, Olomouc – Holice (Czech Republic)
E-mail: alexander.domling@upol.cz
[c] Prof. N. Reiling
RG Microbial Interface Biology, Research Center Borstel
Leibniz Lung Center, Parkallee 1–40, Borstel 23845 Sülfeld (Germany)
E-mail: nreiling@fz-borstel.de
[d] Prof. N. Reiling
German Center for Infection Research (DZIF)
Partner Site Hamburg-Lübeck-Borstel-Riems
Borstel 23845 Greifswald (Germany)

Supporting information for this article is available on the WWW under https://doi.org/10.1002/cmdc.202300279

described under a two-state model: a low substrate affinity (T) state, also known as the constrained or tense state, and a high substrate affinity (R) state, also known as the relaxed state.[14] During the reaction, ATCase changes its conformation from the T state to R state, accompanied by the relative motion of the CP and L-Asp binding domains.[15] N-(Phosphonacetyl)-L-aspartate (PALA), a stable analogue of the transition state intermediate, was synthesized by Collins and Stark in the 1970 s.[16] PALA was reported to be a highly potent and specific transition-state inhibitor of aspartate transcarbamoylase in *Escherichia coli* possessing high activity and low toxicity, demonstrated both *in vitro* and *in vivo*.[17]

ATCase from *Plasmodium falciparum* (*Pf*ATCase) was also identified to be a putative drug target[18] since the malaria parasite is dependent on the *de novo* pyridine biosynthesis pathway during proliferation. High resolution crystals of *Pf*ATCase were used in our previous work to perform fragment screening.[19] Merging the determined fragments allowed the development of a series of compounds with promising inhibition against *Pf*ATCase.[20] Critically, these compounds exploited a previously undescribed allosteric site of *Pf*ATCase, allowing species selectivity between *Plasmodium falciparum* and the human host. Such selectivity is potentially not achievable by PALA, due to sequence conservation of the active site. However, while PALA is known to inhibit the ATCases of various organisms, including humans and *E. coli*, no data on the inhibition of *Mtb*ATCase by PALA is available in the literature.

With the availability of the genome sequence of Mtb,[21] the pyrimidine biosynthesis pathway could be evaluated as an essential pathway for mycobacterial survival,[22] with ATCase shown to be essential for growth.[23] In this manuscript, we assessed the inhibition of ATCase from *Mycobacterium tuberculosis* (*Mtb*ATCase) by the compound series developed against *Pf*ATCase (the BDA series). Based on *in vitro* activity assays, these compounds are able to distinguish between *Pf*ATCase, *Human* ATCase and *Mtb*ATCase. Our results also demonstrated that members of the BDA series showed inhibition for *Mtb*ATCase in the single digit μM range with noncompetitive inhibition. Interestingly, control experiments using PALA show no inhibition. The most potent inhibitors were further screened in a MIC_{90} assay on *M. tuberculosis* cell cultures, with BDA-06 demonstrating a MIC_{90} of 4 μM. Molecular modelling experiments demonstrate that the *Mtb*ATCase has a similar pocket to that shown on *Pf*ATCase, further supporting the hypothesis that these compounds may act allosterically on *Mtb*ATCase.

Results and Discussion

A 70-member library of ATCase inhibitors, known to be designed and active against the *Pf*ATCase (the BDA series), was screened in an *in vitro* enzymatic assay against *Mtb*ATCase (Figure 1A). This series of compounds were designed based on the core scaffold of BDA-01, varying functional groups to optimize inhibition. The half maximal inhibitory concentration (IC_{50}) was measured using the absorbance of the product, carbamoyl-aspartate at 466 nm. The results of the activity assays demonstrated that most of BDA series showed inhibition in the high μM range. However, a smaller number of compounds displayed IC_{50} values in the single digit μM range. BDA-06, −10, −14, −17, −25, −54, −63, −67, −69 and −70 displayed promising IC_{50} values of 1.44 μM, 6.89 μM, 2.05 μM, 6.01 μM, 6.13 μM, 3.54 μM, 3.60 μM, 6.98 μM, 3.49 μM and 1.36 μM, respectively (Figure 1B). Compared to the core structure (Figure S1), most of these 10 compounds retain both aromatic groups (Figure S1, R^1) add a tert-butyloxycarbonyl protecting group (BOC group) to the amino group (Figure S1, R^3), and vary the methoxy group (Figure S1, R^2), with the exception of BDA-67 and BDA-70. In addition, BDA-67 and BDA-69 retain a methoxy group also with promising IC_{50} values, especially BDA-67, replacing 5-phenyl group with 4,5-tetrahydrobenzo. In addition, we performed the active assay using PALA, with the results showing that PALA surprisingly has no inhibition under our assay conditions (Figure 1C). In a follow-up experiment, the 4 most potent inhibitors were also screened against *Pf*ATCase and human ATCase[20] (Figure 1D). These results again demonstrate species selectivity of this compound series. Overall, while the inhibition of *Mtb*ATCase is weaker for these 4 compounds, our results do provide the first demonstration of an *Mtb*ATCase inhibitor, as the canonical ATCase inhibitor PALA showed no inhibition at concentrations under 100 μM (Figure 1C), whereas BDA-06 displays an IC_{50} of 1.44 μM. These results suggest that further optimization of the BDA series, with a focus on *Mtb*, rather than *P. falciparum* may yield compounds able to selectively inhibit *Mtb*ATCase without affecting the activity of the ATCase of the human host.

As it is known that the BDA series inhibit the *Pf*ATCase allosterically, we decided to evaluate the hypothesis that a similar pocket and mechanism may exist in *Mtb*ATCase and thereby understand the binding of BDA series compounds to *Mtb*ATCase. Firstly, the hypothesis of a non-competitive mechanism was assessed, with an enzyme activity assay at different concentrations of an exemplar (BDA-06) with varying concentrations of Asp or CP performed. The results are in accordance with the Michaels-Menten equation, which indicates the non-competitive inhibition of BDA-06 (Figure 1E&1F). Since the structure of MtbATCase is currently unavailable, we performed a structure prediction of *Mtb*ATCase using the *Plasmodium falciparum* (*P. falciparum*) ATCase apo structure (T-state; PDB: 5ILQ) and citrate complex structure (R-state; PDB:5ILN) as templates with the SWISS MODEL server[24] (Figure 2A). The sequence identity and conservation between the *Pf*ATCase and *Mtb*ATCase are 27% and 66% over 319 residues, respectively. The residues of the proposed inhibitor binding site are highly conserved, with 8 out of 11 residues within 3.5 Å of the experimentally determined binding site of BDA-04 with *Pf*ATCase (PDB: 7zp2) absolutely conserved (Figure S2). The resulting models indicated that the *Mtb*ATCase T-state may have a similar pocket to that seen on *Pf*ATCase (Figure 2B). As expected, this pocket is absent in the R-state *Mtb*ATCase model. These models also suggest that a loop comprising residues 77–89 to be highly flexible (Figure 3A), similarly to the 120 loop of *Pf*ATCase. The apo *Mtb*ATCase structural model was further analyzed by FTMap,[25] to identify binding hot spots of macromolecules. The

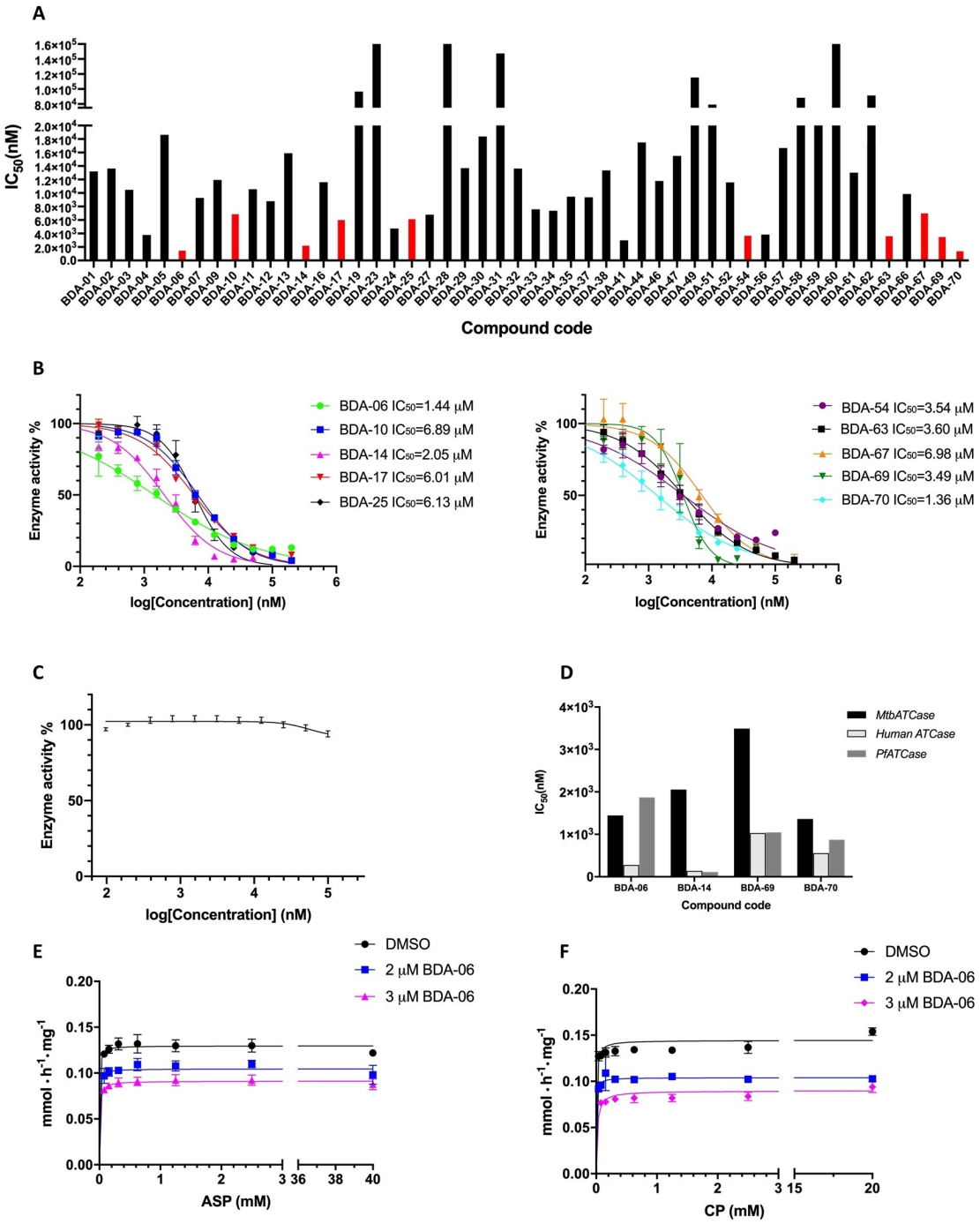

Figure 1. The BDA compound series inhibits *Mtb*ATCase *in vitro.* A) IC_{50} values of an enzymatic assay of BDA series compounds (70 compounds) against *Mtb*ATCase. Only compounds showing a measurable IC_{50} are displayed. Compounds taken forward are highlighted in red; B) IC_{50} values of an enzymatic assay of selected compounds BDA −06, −10, −14, −17, −25, −54, −63, −67, −69 and −70 compounds against *Mtb*ATCase repeated in triplicate are shown; C) An enzymatic assay of PALA against *Mtb*ATCase indicates no inhibition; D) A comparison of an enzymatic IC_{50}s for the best 4 *Mtb*ATCase inhibitors against *Mtb*ATCase, *Pf*ATCase and *Human* ATCase demonstrating species selectivity; E&F) Enzymatic assay at different concentrations of BDA-06, fixed CP concentration (25 mM) with varying Asp concentration (E), or fixed Asp concentration (20 mM) with varying CP concentration (F).

results showed that the identified pocket is indeed available to the solvent for macromolecule binding (Figure S3). Finally, we predicted a model of the BDA-06:*Mtb*ATCase complex using the software *smina*,[26] which indicated that BDA-06 could occupy the predicted allosteric pocket of T-state *Mtb*ATCase (Figure 3B&3C). The docking results predict that the sulfamoylbenzyl group of BDA-06 is buried in the allosteric pocket, and the phenylthiophene group partially occludes the CP binding domain in a manner similar to that seen in the experimental structure of *Pf*ATCase with BDA-04. Further, other BDA series

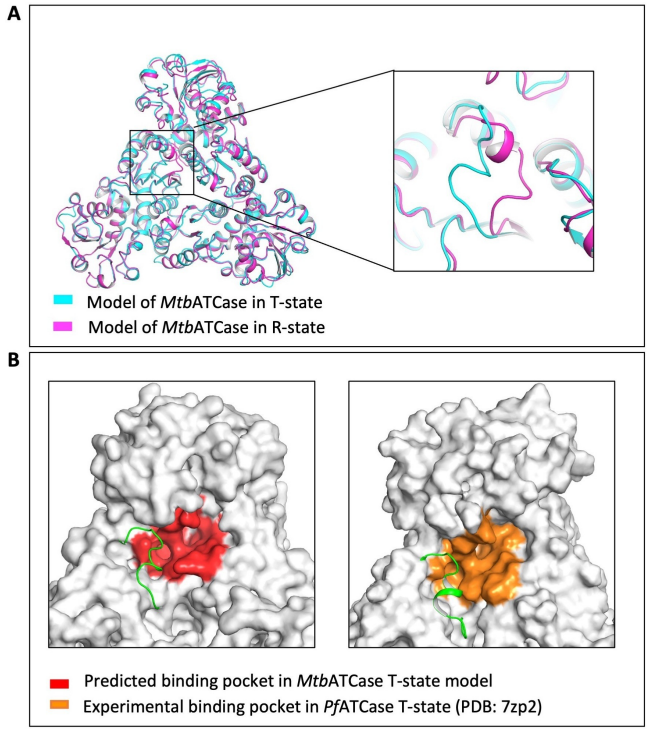

Figure 2. Structure prediction of *Mtb*ATCase. A) Structure prediction of *Mtb*ATCase suggests that an allosteric pocket may exist, similarly to that seen in *Pf*ATCase. The structure of *Mtb*ATCase was predicted based on the homologous structures from *P. falciparum*. The model created from the apo state (T-state) of *P. falciparum* is shown in blue, and that created from *the Pf*ATCase:citrate complex (R-state) of *P. falciparum* in purple; B) The potential binding pocket from the apo state of *Mtb*ATCase is shown in red, with the equivalent pocket of *Pf*ATCase is shown in orange. The flexible loop of *Mtb*ATCase and 120 loop of *Pf*ATCase highlighted in green.

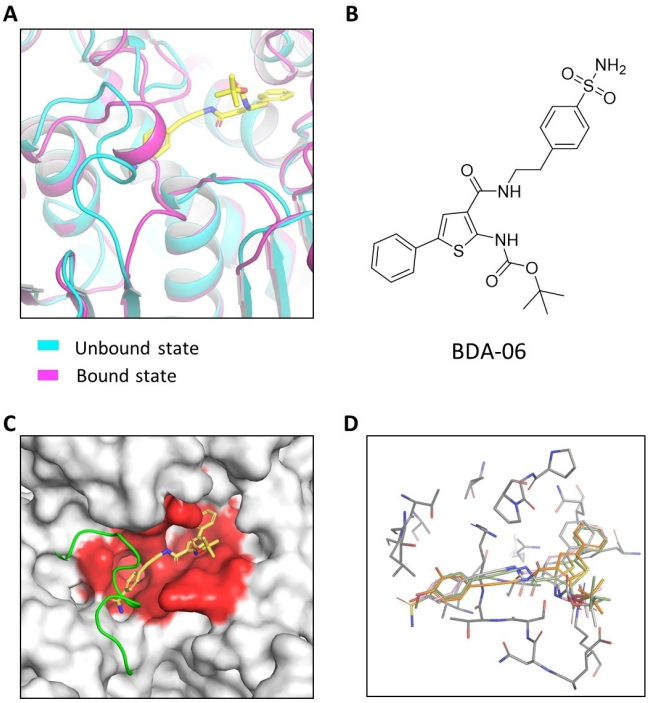

Figure 3. Models of the *Mtb*ATCase:BDA-06 complex. A) Binding of BDA-06 can be accommodated in *Mtb*ATCase models generated from both the apo- (T-state; blue) but not R-state (purple) forms of *P. falciparum* B) structure of BDA-06; C) Surface representation of apo-*Mtb*ATCase showing that BDA-06 can be accommodated in the proposed binding pocket (highlighted as in Figure 2B); D) Stick mode of predicted binding pocket of apo-*Mtb*ATCase in complex with BDA-06, 11, 25 and 29, carbon atoms of predicted binding pocket shown in grey, BDA-06 shown in white, BDA-11 shown in pink, BDA-25 shown in orange and BDA-29 shown in green, respectively.

compounds containing a phenylthiophene group (BDA-11, 25 and 29) also showed similar docking results, occupying the same pocket (Figure 3D).

The 10 best performing compounds of the enzymatic assay underwent further analysis. First, the solubility of the compounds in the Mtb growth assay medium (7H9 + 10 %OADC) was addressed by Dynamic Light Scattering using a Zetasizer. The results showed that all compounds were soluble at concentrations up to 8 μM (Figure S4). Anti-TB activity of the compounds was then analyzed by fluorescence measurements in head-to-head comparison at 8 μM employing *Mtb* H37Rv bacteria expressing mCherry10 fluorescent protein, using the antibiotic Rifampicin as a positive control (Figure 4A). This identified BDA-06 as the most active of the tested compounds.

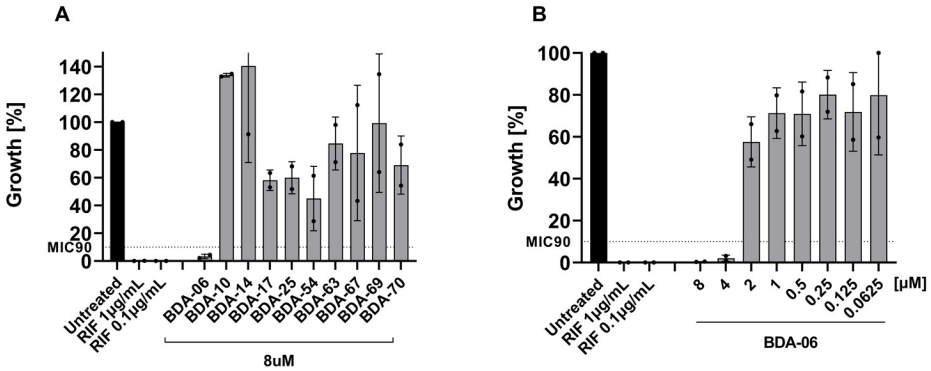

Figure 4. Impact of the BDA compound series on Mtb bacterial growth in liquid culture. A) Head-to-head comparison of anti-mycobacterial activity (MIC_{90}) of compounds BDA-06, −10, −14, −17, −25, −54, −63, −67, −69 and −70 (all at 8 μM) using mCherry10 expressing Mtb H37Rv bacteria; B) Dose-response MIC_{90} assay of BDA-06 indicates a MIC_{90} of 4 μM.

The MIC_{90} was then determined in titration experiments (Figure 4B), indicating that BDA-06 possesses a MIC_{90} of 4 μM. Initial host cell cytotoxicity assays using human monocyte derived macrophages (hMdM) and 1% Triton-X 100 as a positive control, identified a cytotoxic concentration 50 (CC_{50}) for BDA-06 of approximately 30 μM (Figure S5A&S5B).

Conclusions

Our previous work had demonstrated the existence of an allosteric pocket in the ATCase of *P. falciparum*.[20] The sequence variation in this pocket has already been shown to allow for selectivity between the malarial parasite and its human host. Further, these compounds reduced parasite proliferation, likely through an inhibition of the pyrimidine biosynthesis pathway. Based on these results were hypothesized that the library of compounds developed for the inhibition of *Pf*ATCase may also contain inhibitors of ATCases of other organisms and that inhibition of pyrimidine biosynthesis may also provide a mechanism to address other infectious diseases, such as tuberculosis. The data presented in this manuscript demonstrate that this compound library indeed contains a number of *in vitro* inhibitors of *Mtb*ATCase. Given that the classical ATCase inhibitor PALA showed no significant inhibition of *Mtb*ATCase, this report contains the first demonstration of inhibitors of *Mtb*ATCase. This lack of inhibition of *Mtb*ATCase by the transition state analogue PALA suggests that access to the catalytic site of *Mtb*ATCase may be distinct in *M. tuberculosis* from that seen in previous organisms, such as *E. coli* and humans. This is supported by the relative lack in sequence identify of the ATCases of these organisms allowing for slightly divergent reaction mechanisms (47% *Mtb:E. coli*; 37% *Mtb*: Human).

The discovery that a number of compounds from the BDA series also act as inhibitors of *Mtb*ATCase *in vitro* also suggests that such inhibition may be supported by a similar allosteric mechanism as seen for inhibition of *Pf*ATCase. This is supported both by the demonstrated selectivity of BDA-6, −14, −69 and −70 (Figure 1D) that suggests a degree of sequence variation around the binding site for these molecules and the kinetic assays that strongly suggest a non-competitive mode of inhibition (Figures 1E&1F). While our results do also indicate stronger inhibition of the *human* ATCase by these compounds it should be borne in mind that this series has not yet been optimized for activity against the tubercular enzyme.

The most potent of the compounds tested *in vitro* were then assessed for their activity against *M. tuberculosis* cells in culture, with BDA-06 displaying a MIC_{90} of 4 μM. While our data cannot positively identify *Mtb*ATCase as the target of BDA-06 inhibition in these assays, these experiments do suggest that inhibition of pyrimidine biosynthesis may provide an attractive target for further drug development. The relative lack of inhibition of hMdM (CC_{50} 30 μM) also again suggests that the reliance of proliferating cells on pyrimidine biosynthesis rather than salvage pathways may further strengthen the argument for addressing pyrimidine biosynthesis in parasitic diseases. Further experiments to identify the cellular target of BDA-06 and further development of the BDA series to improve inhibitory properties are required. Structural analysis of the BDA-06 binding mode is also required to demonstrate both an allosteric mode of inhibition as well as provide information for compound optimization. The homology modeling experiments reported do support the hypothesis that an allosteric pocket exists on *Mtb*ATCase, which can be further exploited.

Experimental Section

Activity assay

Enzymatic reactions were performed in a total volume of 150 μL in 50 mM Tris-Acetate buffer at pH 8.0 and a final concentration of *Mtb*ATCase of 50 nM. A complete description of the synthesis of the BDA compound series is provided in Wang's manuscript.[20] The concentrations of L-Aspartate (Asp) and carbamoyl-phosphate (CP) were 20 mM and 25 mM. The concentration of BDA series compounds and PALA in dose-response experiments started from 100 μM with 2% (v/v) DMSO. *Mtb*ATCase was pre-incubated with Asp and compounds for 10 min in a shaker at room temperature, then CP was added and incubated for 5 min, the reaction was stopped by adding 100 μL of the colorimetric chemical mixture[27] (two volumes of Antipyrine in 50% (v/v) sulfuric acid and one volume of 2,3-Butanedione monoxime in 5% (v/v) acetic acid). Then the plate was incubated overnight in the dark at room temperature, followed with denaturation at 368 K for 15 min, samples were then measured at 466 nm using a Synergy H1 Hybrid Reader (BioTek).

Solubility measurement by DLS assay

Compounds were analyzed for solubility in 7H9 complete medium (BD Difco; Becton Dickinson; culture medium), supplemented with oleic acid-albumin-dextrose-catalase (OADC, 10%; BD) using the Dynamic Light Scattering (DLS) assay on a Zetasizer Nano ZS90 (Malvern Instruments Ltd, Worcestershire, UK). Analyses were performed in a 100 μl format using disposable cuvettes (67.758, Sarstedt AG & Co, Nümbrecht, Germany) of the compound diluted in culture medium as indicated. Culture treated with DMSO but free of compounds was used as control. The derived count rate values obtained from the analyses indicated the degree of aggregation formation. The values were compared to DMSO treated control sample which allowed the determination of the sample concentration at which the respective compound was entirely soluble, with no detectable aggregate formation.

Determination of in vitro anti-tubercular activity

Anti-tubercular tests were performed as previously described.[28] In brief, 7H9 complete medium (BD Difco; Becton Dickinson, Maryland, USA) supplemented with 10% OADC (BD), 0.2% glycerol, and 0.05% Tween80 as previously described[29] was used to culture *Mycobacterium tuberculosis* (Mtb) strain H37Rv (ATCC 25618) carrying a mCherry-expressing plasmid (pCherry10)[30] Cultures were harvested at mid-log phase and frozen in aliquots at 193 K. Prior to testing aliquots were thawed followed by centrifugation and the pellet was resuspended in 7H9 medium with 10% OADC (without glycerol and Tween80). This was further thoroughly resuspended by passing it through a syringe with a 26-gauge needle to avoid clumping of the bacteria. 2×10^5 CFU were then cultured in a total volume of 100 μl culture medium (triplicates) to test the non-

precipitating compounds for the anti-tubercular activity at the concentrations indicated. For these assays, 96-well flat clear bottom black polystyrene microplates (Corning® CellBIND®, Merck, New York, USA) were used. Each plate had Rifampicin (at 1 μg/ml and 0.1 μg/ml) (National Reference Center, Borstel) as a reference compound. Plates were sealed with an air-permeable membrane (Porvair Sciences, Wrexham, UK) in a 310 K incubator with mild agitation (TiMix5, Edmund Bühler, Germany). The activity of compounds was determined after 7 days by measuring the bacterial growth as relative light units (RLU) from the fluorescence intensity obtained at an excitation wavelength of 575 nm and an emission wavelength of 635 nm in a microplate reader (Synergy 2, BioTek Instruments, Vermont, USA). Two independent experiments (each in triplicates) were performed, and all values were normalized to untreated control sample (100%) in each experiment. The graphs were obtained by the average of both experiments using GraphPad Prism version 9.4.1 for Windows (GraphPad Software, San Diego, California USA, www.graphpad.com). The first concentration of compounds at which 90% Mtb inhibition was observed was considered to be MIC_{90}.

Measurement of in vitro cytotoxicity by XTT assay

An XTT assay was used to determine the cytotoxicity of the compound BDA-06. Human Monocyte-derived Macrophages (hMdM) were differentiated from peripheral blood mononuclear cells (PBMC) of healthy volunteers and cultured as previously described.[31] 5×10^4 cells/well in RPMI medium containing 10% (v/v) heat-inactivated Fetal Bovine Serum and 2 mmol/L l-glutamine (Biochrom, Berlin, Germany) were seeded in presence of 2-fold dilution concentrations (64 μM to 1 μM) of the compound for 24 hours with a final volume of 200 μl/well. For this assay, 96-well clear flat bottom plates (Nunclon™ Delta Surface, ThermoScientific, Denmark) were used. Triton™-X 100 (Sigma-Aldrich, Missouri, USA; 1% in RPMI medium) was used as a positive control. Cells were incubated with 200 μl of Triton-X 100 and incubated for 10 min at 310 K. XTT dye from the kit (SERVA Electrophoresis GmbH; 50 μl) was added to each well and resuspended thoroughly and further incubated for 3–4 hours at 310 K. Subsequently, absorbance values were measured at 490 nm on a multi-well plate reader (Synergy 2, BioTek Instruments, Vermont, USA). Untreated cells were used as negative control. The Cytotoxic Concentration 50 (CC_{50}) was determined by plotting a curve using GraphPad Prism version 9.4.1.

Supporting Information

Additional references cited within the Supporting Information.[32–34]

Acknowledgements

The authors acknowledge financial support from the Chinese Scholarship Council (Xiaochen Du, Bidong Zhang & Chao Wang). The authors also thank Ms. Carolin Golin, Borstel for expert technical support.

Conflict of Interests

The authors have submitted a patent application on the molecules described in the manuscript (21211903.6).

Data Availability Statement

The data that support the findings of this study are available from the corresponding author upon reasonable request.

Keywords: *Mycobacterium tuberculosis* · pyrimidine biosynthesis · aspartate transcarbamoylase · molecular docking · allosteric inhibition

[1] M. C. Gutierrez, S. Brisse, R. Brosch, M. Fabre, B. Omais, M. Marmiesse, P. Supply, V. Vincent, *PLoS Pathog.* **2005**, *1*, e5.
[2] a) G. Delogu, M. Sali, G. Fadda, *Mediterr J Hematol Infect Dis.* **2013**, *5*, e2013070; b) R. Hershberg, M. Lipatov, P. M. Small, H. Sheffer, S. Niemann, S. Homolka, J. C. Roach, K. Kremer, D. A. Petrov, M. W. Feldman, S. Gagneux, *PLoS Biol.* **2008**, *6*, e311.
[3] World Health Organization Global Tuberculosis report 2020.
[4] C. B. Scarim, R. Lira de Farias, A. Vieira de Godoy Netto, C. M. Chin, J. Leandro Dos Santos, F. R. Pavan, *Eur. J. Med. Chem.* **2021**, *214*, 113166.
[5] Z. Lou, Z. Zhang, *Protein Cell.* **2010**, *1*, 435–442.
[6] S. D. Yelamnchi, A. Mishra, S. K. Behra, G. Karthikkeyan, T. S. Keshava P-rasd, A. Surolia, *Metabolites* **2022**, *12*.
[7] A. Aubry, X. S. Pan, L. M. Fisher, V. Jarlier, E. Cambau, *Antimicrob. Agents Chemother.* **2004**, *48*, 1281–1288.
[8] A. Quémard, J. C. Sacchettini, A. Dessen, C. Vilcheze, R. Bittman, W. R. Jacobs Jr, J. S. Blanchard, *Biochemistry* **1995**, *34*, 8235–8241.
[9] V. E. Escuyer, M. A. Lety, J. B. Torrelles, K. H. Khoo, J. B. Tang, C. D. Rithner, C. Frehel, M. R. McNeil, P. J. Brennan, D. Chatterjee, *J. Biol. Chem.* **2001**, *276*, 48854–48862.
[10] L. Kremer, J. D. Douglas, A. R. Baulard, C. Morehouse, M. R. Guy, D. Alland, L. G. Dover, J. H. Lakey, W. R. Jacobs Jr., P. J. Brennan, D. E. Minnikin, G. S. Besra, *J. Biol. Chem.* **2000**, *275*, 16857–16864.
[11] P. LeMagueres, H. Im, J. Ebalunode, U. Strych, M. J. Benedik, J. M. Briggs, H. Kohn, K. L. Krause, *Biochemistry* **2005**, *44*, 1471–1481.
[12] Y. Zhang, *Annu. Rev. Pharmacol. Toxicol.* **2005**, *45*, 529–564.
[13] I. Chitrakar, D. M. Kim-Holzapfel, W. Zhou, J. B. French, *J. Struct. Biol.* **2017**, *197*, 354–364.
[14] a) J. Monod, J. Wyman, J. P. Changeux, *J. Mol. Biol.* **1965**, *12*, 88–118; b) G. J. Howlett, M. N. Blackburn, J. G. Compton, H. K. Schachman, *Biochemistry* **1977**, *16*, 5091–5099.
[15] J. R. Wild, S. J. Loughrey-Chen, T. S. Corder, *Proc. Natl. Acad. Sci. USA* **1989**, *86*, 46–50.
[16] K. D. Collins, G. R. Stark, *J. Biol. Chem.* **1971**, *246*, 6599–6605.
[17] a) R. K. Johnson, T. Inouye, A. George, G. R. Stark, *Cancer Res.* **1976**, *36*, 2720–2725; b) E. A. Swyryd, S. S. Seaver, G. R. Stark, *J. Biol. Chem.* **1974**, *249*, 6945–6950.
[18] W. Sun, T. Q. Tanaka, C. T. Magle, W. Huang, N. Southall, R. Huang, S. J. Dehdashti, J. C. McKew, K. C. Williamson, W. Zheng, *Sci. Rep.* **2014**, *4*, 3743.
[19] S. Lunev, S. S. Bosch, A. Batista Fde, C. Wrenger, M. R. Groves, *Acta Crystallogr., Sect. F: Struct. Biol. Commun.* **2016**, *72*, 523–533.
[20] C. Wang, B. Zhang, A. Kruger, X. Du, L. Visser, A. S. S. Domling, C. Wrenger, M. R. Groves, *J. Am. Chem. Soc.* **2022**, *144*, 19070–19077.
[21] S. T. Cole, R. Brosch, J. Parkhill, T. Garnier, C. Churcher, D. Harris, S. V. Gordon, K. Eiglmeier, S. Gas, C. E. Barry III, F. Tekaia, K. Badcock, D. Basham, D. Brown, T. Chillingworth, R. Connor, R. Davies, K. Devlin, T. Feltwell, S. Gentles, N. Hamlin, S. Holroyd, T. Hornsby, K. Jagels, A. Krogh, J. McLean, S. Moule, L. Murphy, K. Oliver, J. Osborne, M. A. Quail, M.-A. Rajandream, J. Rogers, S. Rutter, K. Seeger, J. Skelton, R. Squares, S. Squares, J. E. Sulston, K. Taylor, S. Whitehead, B. G. Barrell, *Nature* **1998**, *393*, 537–544.
[22] D. F. Warner, J. C. Evans, V. Mizrahi, *Microbiol. Spectrum* **2014**, *2*.
[23] C. M. Sassetti, D. H. Boyd, E. J. Rubin, *Mol. Microbiol.* **2003**, *48*, 77–84.

[24] T. Schwede, J. Kopp, N. Guex, M. C. Peitsch, *Nucleic Acids Res.* **2003**, *31*, 3381–3385.
[25] D. Kozakov, L. E. Grove, D. R. Hall, T. Bohnuud, S. E. Mottarella, L. Luo, B. Xia, D. Beglov, S. Vajda, *Nat. Protoc.* **2015**, *10*, 733–755.
[26] D. R. Koes, M. P. Baumgartner, C. J. Camacho, *J. Chem. Inf. Model.* **2013**, *53*, 1893–1904.
[27] S. C. Pastra-Landos, J. Foote, E. R. Kantrowit, *Anal. Biochem.* **1981**, *118*, 358–363.
[28] R. P. Jumde, M. Guardigni, R. M. Gierse, A. Alhayek, D. Zhu, Z. Hamid, S. Johannsen, W. A. M. Elgaher, P. J. Neusens, C. Nehls, J. Haupenthal, N. Reiling, A. K. H. Hirsch, *Chem. Sci.* **2021**, *12*, 7775–7785.
[29] K. Kolbe, L. Möckl, V. Sohst, J. Brandenburg, R. Engel, S. Malm, C. Brauchle, O. Holst, T. K. Lindhorst, N. Reiling, *ChemBioChem* **2017**, *18*, 1172–1176.
[30] A. Zelmer, P. Carroll, N. Andreu, K. Hagens, J. Mahlo, N. Redinger, B. D. Robertson, S. Wiles, T. H. Ward, T. Parish, J. Ripoll, G. J. Bancroft, U. E. Schaible, *J. Antimicrob. Chemother.* **2012**, *67*, 1948–1960.
[31] N. Reiling, S. Homolka, K. Walter, J. Brandenburg, L. Niwinski, M. Ernst, C. Herzmann, C. Lange, R. Diel, S. Ehlers, S. Niemann, *mBio* **2013**, *4*.
[32] A. Dummler, A. M. Lawrence, A. de Marco, *Microb. Cell Fact.* **2005**, *4*, 34.
[33] D. G. Gibson, L. Young, R.-Y. Chuang, J. C. Venter, C. A. Hutchison, H. O. Smith, *Nat. Methods* **2009**, *6*, 343–345.
[34] D. Kozakov, L. E. Grove, D. R. Hall, T. Bohnuud, S. E. Mottarella, L. Luo, B. Xia, D. Beglov, S. Vajda, *Nat. Protoc.* **2015**, *10*, 733–755.

Manuscript received: May 24, 2023
Revised manuscript received: June 7, 2023
Accepted manuscript online: June 9, 2023
Version of record online: June 30, 2023